Evolutionary Systematics. 9 2025, 87–98 | DOI 10.3897/evolsyst.9.143758

PENSOFT

EVOLUTIONARY SYSTEMATICS

A new species and the phylogenetic placement of the Neotropical genus *Gephyrellula* Strand, 1932 (Araneae, Philodromidae)

Hector Baruch Pereira Schinelli[1,2], André Wanderley do Prado[3], Renner Luiz Cerqueira Baptista[1], Daniela Maeda Takiya[4]

1 *Laboratório de Diversidade de Aracnídeos, Departamento de Zoologia, Instituto de Biologia, Universidade do Brasil/Universidade Federal do Rio de Janeiro, Av. Carlos Chagas Filho 373, 21941-902, Cidade Universitária, Rio de Janeiro, RJ, Brazil*

2 *Programa de Pós-graduação em Zoologia, Museu Nacional, Rio de Janeiro, Brazil*

3 *Harry Butler Institute, Murdoch University, Building 390, Level 4, 90 South St, Murdoch WA 6150, Australia*

4 *Laboratório de Entomologia, Departamento de Zoologia, Instituto de Biologia, Universidade do Brasil/Universidade Federal do Rio de Janeiro, Av. Carlos Chagas Filho 373, 21941-902, Cidade Universitária, Rio de Janeiro, RJ 21941-902, Brazil*

https://zoobank.org/E9C8E411-7BB7-4A3C-8DAB-9AC0D8C31A49

Corresponding author: Hector Baruch Pereira Schinelli (hectorschinelli@gmail.com)

Academic editor: Stephanie F. Loria ♦ **Received** 6 December 2024 ♦ **Accepted** 14 March 2025 ♦ **Published** 7 April 2025

Abstract

Gephyrellula Strand, 1932 is a genus of small flat pale spiders from the running crab spider family Philodromidae, which currently includes the type-species *Gephyrellula violacea* (Mello-Leitão, 1918), and the recently described *G. lavidabonita* Galvis et al., 2024. The genus has appeared in phylogenetic analyses as a member of the subfamily Philodrominae, but there are conflicting hypotheses regarding its closest relatives. One analysis placed *Gephyrellula* among the Hawaiian genera *Pedinopistha* Karsch, 1880 and *Pagiopalus* Simon, 1900, whereas the other placed it among species of *Philodromus* Walckenaer, 1826. To further investigate the topic, we conducted new phylogenetic analyses using four molecular markers and including two terminals of *Gephyrellula*. The resulting trees support the division of the family into two subfamilies Thanatinae and Philodrominae, with *Gephyrellula* as a member of the latter. Our results place *Gephyrellula* neither as a member of the Hawaiian clade nor among the genus *Philodromus*, but instead as a separated lineage. In addition to the phylogenetic analysis, we describe a new species of the genus named *Gephyrellula condeuba* **sp. nov.**, and provide new records of *G. violacea*, expanding the known distribution of the genus.

Key Words

Running crab spiders, South America, systematics, taxonomy

Introduction

The spider family Philodromidae includes 529 extant species placed in 30 genera (World Spider Catalog 2025), and it comprises active predators known as running crab spiders, usually found on branches and leaves of bushes and small trees, and also in grass, tree bark, rocks and soil litter. Originally described as a subfamily of Thomisidae, they are characterized as small spiders with a flattened body; with a dense, soft recumbent setal covering; eight eyes not placed in tubercles, without tapetum and arranged in two recurved rows; and legs usually with scopulae and similar in size or with leg II longer (Dondale and Redner 1978). Philodromidae was raised to family level by Homann (1975) based on morphological and ontogenetic characters. The family's monophyly has been supported by recent phylogenies, based on both molecular (Wheeler et al. 2017; Griotti et al. 2022; Prado et al. 2022) and morphological characters (Ramírez 2014), and the main synapomorphy for the family is the presence of tenent hairs in both male and female palps. Schick (1965) divided the group in two tribes, Thanatini and

Copyright *Hector Baruch Pereira Schinelli et al.* This is an open access article distributed under the terms of the Creative Commons Attribution License (CC BY 4.0), which permits unrestricted use, distribution, and reproduction in any medium, provided the original author and source are credited.

Philodromini, which have been formally elevated to subfamilies by Prado et al. (2022). The systematics of Neotropical Philodromidae is still poorly studied (Dupérré 2022; Prado et al. 2022). Among the 14 genera cited in the Neotropics (World Spider Catalog 2025), a total of five were taxonomically revised: *Berlandiella* Mello-Leitão, 1929 by Lise and Silva (2011) with additions by Pantoja et al. (2020), *Gephyrellula* Strand, 1932 by Santos and Rheims (2018), *Petrichus* Simon, 1886 by Griotti et al. (2022), *Cleocnemis* Simon, 1886 by Prado et al. (2022) and *Fageia* Mello-Leitão, 1929 by Schinelli et al. (2024).

Gephyrellula was described by Mello-Leitão (1918), as *Gephyrella*, but Strand (1932) noticed that this name was preoccupied in Lepidoptera and established the replacement name *Gephyrellula*. The genus was originally proposed based only on the type-species *Gephyrellula violacea* (Mello-Leitão, 1918), from Pinheiro [currently Pinheiral], Rio de Janeiro state, Brazil. Years later, a new species, *Gephyrellula paulistana* Soares, 1943, was described from São Paulo, São Paulo state, Brazil (Soares 1943). In the revision of the genus (Santos and Rheims 2018), *G. paulistana* was considered a junior synonym of *G. violacea*, turning *Gephyrellula* monotypic again until the recent description of *Gephyrellula lavidabonita* Galvis et al., 2024 from Colombia.

Gephyrellula has been considered to be close to *Gephyrina* Simon, 1895 and *Gephyrota* Strand, 1932 (replacement name for *Gephyra* L. Koch, 1875) (Mello-Leitão 1918, 1929, p. 107, 259; Santos and Rheims 2018). The only phylogenetic analysis to include this genus was the molecular phylogeny by Prado et al. (2022) in their revision of *Cleocnemis*, which placed *Gephyrellula* as a member of Philodrominae. However, the internal position of *Gephyrellula* varied in different analyses and had low support values. In the maximum likelihood tree, the genus was recovered in a clade with the Hawaiian genera, with *Pagiopalus* Simon, 1900 as sister to *Pedinopistha* Karsch, 1880 + *Gephyrellula*. In the Bayesian Inference tree though, the genus was associated with *Philodromus* Walckenaer, 1826, being recovered as sister-group to a clade with "*Cleocnemis*" *mutilata* (Mello-Leitão, 1917) as sister to *Philodromus aureolus* (Clerck, 1757) + *P. cespitum* (Walckenaer, 1802), while *P. spinitarsis* Simon, 1895 was the sister-group to this clade (Prado et al. 2022, fig. 1). One possible reason for the inconsistencies in the different analyses was the lack of data, since only H3, out of the four molecular markers used in that study, was sequenced for *Gephyrellula violacea*.

In this study we describe a new species of *Gephyrellula* from northeastern Brazil, give new records and taxonomic comments for *G. violacea* and amend the genus diagnosis. To help further understand the so far inconsistent phylogenetic relationships of the genus, we also perform new phylogenetic analyses based on data from Prado et al. (2022), including new sequences of the four molecular markers for *G. violacea* as well as *G. condeuba* sp. nov. We then discuss the genus' morphological characters in comparison to its putative closest relatives.

Material and methods

Material examined

Specimens of the new species were collected by beating and sweeping vegetation in Condeúba, Bahia State, Brazil, and were preserved in 90% ethanol. Male holotype and female paratype are deposited in the spider collection of Laboratório de Diversidade de Aracnídeos, Instituto de Biologia, Universidade Federal do Rio de Janeiro (LABAR-UFRJ). Specimens of the new records of *G. violacea* are from the following collections (abbreviation and curator in parentheses): Museo Argentino de Ciencias Naturales "Bernardino Rivadavia", Buenos Aires, Argentina (MACN, M. Ramírez); Museo Nacional de Historia Natural del Paraguay (IBNP, J. Kochalka). Multifocus photographs were obtained with a LEICA M205 C and mounted in LEICA Application Suite Version 4.8.0 software. Illustrations are based on photographs, drawn in Adobe Illustrator 2024 and colored and edited in Adobe Photoshop 2021. Distribution map was created in QGIS 3.16.1 software.

Terminology and abbreviations

Terminology of structures follow Prado et al. (2022). Abbreviations: **ALE**: Anterior Lateral Eyes, **AME**: Anterior Median Eyes, **CG**: Copulatory Guides (= Anterior Guide Pockets *sensu* Santos and Rheims 2018), **GH**: Glandular Head, **GP**: Guide Pockets (= Posterior Guide Pockets *sensu* Santos and Rheims 2018), **MOQ**: Median Ocular Quadrangle, **MS**: Median Septum, **PCA**: Paraconductor Apophysis (= Conductor Process *sensu* Santos and Rheims 2018), **PLE**: Posterior Lateral Eyes, **PME**: Posterior Median Eyes, **RMC**: Retromarginal Conductor (= Conductor *sensu* Santos and Rheims 2018), **RTA**: Retrolateral Tibial Apophysis, **VTA**: Ventral Tibial Apophysis. All measurements are in millimeters.

DNA extraction, amplification, and sequencing

Genomic DNA was extracted using DNeasy blood & tissue kit (Qiagen, Hilden, Germany). The same molecular markers from Prado et al. (2022) and Wheeler et al. (2017) were used for the phylogeny: partial sequence of the Cytochrome Oxidase subunit I (COI), 16S rDNA, 28S rDNA and H3. Markers were amplified using Polymerase Chain Reaction (PCR), with reactions with a total volume of 25 µl, consisting of 12.5 –13.5 µl of H2O, 5.0 µl of PCR buffer GoTaq® Flexi (Promega, Madison, USA), 3 µl of $MgCl_2$ (25 mM, Promega), 0.5 µl of dNTP mix (20 mM, Promega), 1 µl of each forward and reverse primer (10 pmol/l), 0.1 µl of GoTaq® Flexi Polymerase (5U/µl, Promega), and 1–2 µl of DNA extract. Fragments of COI were amplified using the following thermocycling settings: 94 °C for 3 min, followed by 35 cycles at 94 °C for 1 min, 48 °C for 1 min, and 72 °C for 2 min, and a final

extension at 72 °C for 7 min. Fragments of H3, 16S, and 28S were amplified as above, but with an annealing temperature of 50 °C. Amplified products were stained with GelRed® (Biotium, Fremont, USA) and observed under UV light after 1% agarose gel electrophoresis and compared with a molecular weight standard. Successful amplicons were purified with ExoSAP-ITTM (Applied Biosystems, Waltham, EUA) and sent to Macrogen® (South Korea) for Sanger sequencing. Primers used for PCR and sequencing were the same used by Prado et al. (2022). Complementary electropherograms were assembled and edited in GeneStudio v2.2.0. Consensus sequences generated were checked by comparison with similar sequences in GenBank® using BLAST® (Altschul et al. 1990) to verify correct homology or taxonomic contamination. Sequences newly generated herein for *G. violacea* (accessions PV041427, PV077733, PV076735, PV092569) and for *G. condeuba* sp. nov. (accessions PV041426, PV077732, PV076734, PV092568), besides those for outgroup terminals, *Apollophanes gaucho* Francisco et al., 2016 (accessions PV041424, PV077730, PV092566) and *Fageia amabilis* Mello-Leitão, 1929 (accessions PV041425, PV077731, PV076733, PV092567), were deposited in GenBank® (see Suppl. material 1).

Phylogenetic analysis

Phylogenetic analyses were based on DNA sequences of 25 terminals, which were mostly the same as Prado et al. (2022) with some changes. Since that phylogeny was focused on *Cleocnemis* and other Thanatinae, many terminals of species placed in that genus were not considered here as they would not add information to the present work, with focus on *Gephyrellula* and other Philodrominae. Therefore, only two terminals of *Cleocnemis* and two of *Tibelloides* were included in our analyses. The species considered *incertae sedis* were also not included, since this analysis did not aim to position them in either existing or new genera. The uncertain terminals *Thanatus* sp. and Eutichuridae sp. were not included, and the terminal *Apollophanes* sp. was replaced by *Apollophanes gaucho*. *Petrichus* is represented by the previously included *Petrichus* sp. and also by its type-species *P. marmoratus* Simon, 1886 (latter based on data from Griotti et al. [2022]). *Fageia amabilis*, was also included in our analyses.

Multiple alignments were conducted in MAFFT using E-INS for ribosomal markers and Auto for other markers. The concatenated data matrix included 2,400 bp (COI: 543, 16S: 342, 28S: 1,221, H3: 294). Maximum likelihood (ML) analyses were performed on the concatenated matrix in IQ-TREE 2.3.5 (Nguyen et al. 2015) with partitions for each marker and for each codon position of coding genes (total of eight initial partitions), with the best evolutionary model and partition scheme selected by BIC (Schwarz 1978) in ModelFinder (Kalyaanamoorthy et al. 2017). Selected scheme with five partitions were as follows: 16S, COI pos1, COI pos3, H3 pos3, and 28S + COI pos2 + H3 pos1 + H3 pos 2. Clade support was inferred through 1,000 replicates of approximate likelihood ratio test with the nonparametric Shimodaira-Hasegawa correction (SH-aLRT, Anisimova et al. 2011) and ultrafast bootstrap (UFBoot, Hoang et al. 2018). For Bayesian inference (BI), the best evolutionary model was also selected by the same method explained above, but limiting the search for only models that can be implemented in MRBAYES. The analysis of the concatenated matrix was performed in MRBAYES 3.2.7 (Ronquist et al. 2012) through two independent searches, each with four Markov chains, for 50,000,000 generations, saving a tree every 5,000 generations. Of these, 12,500,000 generations were considered burn-in, corresponding to 12,501 trees. All analyses showed adequate convergence of independent analyses and parameter mixing, which were assessed by average standard deviation of split frequencies <0.005, parameter Potential Scale Reduction Factor $=1.00$, and ESS values $>10{,}000$. Clade support of BI analysis is shown by Bayesian posterior probabilities (PP).

Results

Taxonomy

Family Philodromidae Thorell, 1869

Gephyrellula Strand, 1932

Figs 1–4

Gephyrella Mello-Leitão, 1918: 121; Mello-Leitão 1929: 107, 259, 261.

Gephyrellula Strand, 1932: 137 (replacement name for *Gephyrella* Mello-Leitão, preoccupied in Lepidoptera).

Gephyrellula: Soares, 1943: 10; Santos and Rheims 2018: 382.

Diagnosis. *Gephyrellula* may be recognized by the carapace flat and wider than long, with a marginal row of anteriorly directed bristles, relatively low clypeus, median eyes of both rows closer to lateral ones than to the other, all eyes with white veil, and lack of leg scopula. Males have palps bearing a small hook-shaped PCA, well developed VTA and RTA, with RTA more sclerotized than VTA, small and almost inconspicuous RMC (present in *G. violacea*, but doubtful in *G. condeuba* sp. nov.), and long curved embolus starting at prolateral margin of bulb, bordering anterior margin and pointing towards the palp tibia. Females have epigyne simple, wider or as wide as long, MS variable, usually wider than long (longer than wide in *G. lavidabonita*), wider at anterior margin (wider at middle portion in *G. lavidabonita*), and lateral plates projected in a thin, acutely pointed, elevated median lobe (no projected point in *G. lavidabonita*), separating the CG and the GP, and the GH stalk inserted near the middle or at the posterior region of spermatheca, not near its anterior margin.

Description. Males: total length: 3.0–4.2; carapace length: 1.1–1.6; females: total length: 3.5–6.2;

carapace length: 1.2–2.1. Carapace pale to dark yellow with a lighter triangle pointing to fovea, many suffused with dark dots or irregular spots denser near lateral margins. Males typically darker with bigger and denser spots, females may have white pigments at lateral and/or posterior margin. Carapace wider than long, wider at legs II or III; with rows of strong bristles along lateral margins facing anteriorly (visible in Santos and Rheims 2018, fig. 15). Chelicerae with same color and pattern as carapace, longer than wide; fangs same color as paturon; small teeth. Endites same color or a little darker than sternum; labium a little darker than both. Labium wider than long with anterior margin rounded; endites longer than wide, oblong, angled inwards. Sternum pale yellow with much fewer dark spots than on carapace or none at all; anterior margin slightly concave; posterior margin round and convex, separating coxae IV by 1.0 to 1.5 times their width. Eyes with white veils placed in two recurved rows, posterior more recurved than anterior; PME closer to PLE than to each other; eyes near equal in size but AME and/or PLE a little larger than ALE and PME.

Legs with spot patterns similar to carapace but often denser, sometimes making areas appear almost uniformly dark, but lighter venter. Leg II almost always the longest, but leg I longer than II at least in female paratype of *G. condeuba* sp. nov.; leg IV shortest. Spination pattern variable. Usually tibiae bear 2 or 3 pairs or ventral spines and metatarsi 3 pairs; patellae and tarsi without spines; females usually have almost or none spines on femora.

Abdomen with guanine spots covering most of dorsum and/or dark spots usually denser near laterals; cardiac mark visible but not strongly delimited or pigmented. Shape oval with acute posterior end and a notch of variable depth on anterior margin. Two pairs of conspicuous dorsal sigillae, the second one elongated and subdivided; followed by two pairs of smaller depressions in the end of the median third. Venter lighter than dorsum; spinnerets pale yellow, conical.

Male palp with tibia longer than wide; RTA relatively small, well sclerotized, forming a broad rounded or a thin pointed lobe, with 1 to 2 acute tips; VTA relatively large, forming a transversal lobe placed near or closely pressed to the RTA, lightly sclerotized. Tegulum elliptic, weakly projected ventrally; tegular suture clearly seen and long, placed at basal third of tegulum and separating the long median loop of reservoir; PCA small, hook-shaped; primary membranous conductor lacking; RMC small and almost inconspicuous (present in *G. violacea*, but doubtful in *G. condeuba* sp. nov.); embolus originating from the apical third of the prolateral margin of tegulum; relatively long, semicircular, tapering towards a thinner tip, which is pointed towards palpal tibia. Embolus tip pressed against the RMC at the retrolateral distal margin of cymbium. Female epigyne simple, wider or as wide as long; MS variable, usually wider than long (longer than wide in *G. lavidabonita*), wider at anterior margin (wider at middle portion in *G. lavidabonita*); lateral plates usually projected in a thin, acutely pointed, elevated median lobe (no projected lobe and MS covering the posterior region of the lateral plates in *G. lavidabonita*); CG semicircular, anteriorly placed, usually separated from the GP by the lateral plate lobe (CG with posterior portion covered by lateral plates and no GP in *G. lavidabonita*); main spermatheca globose to piriform; GH placed ectally and clearly surpassing the anterior margin of spermatheca, globose (except *G. condeuba* sp. nov.), with long and curved stalk inserted near the middle or at the posterior region of spermatheca, not near its anterior margin.

Taxonomic notes. A comparative diagnosis of *Gephyrellula* and similar genera is included in the Discussion section, with comments on previous works and on the phylogenetic placement of the genus.

Composition. *Gephyrellula violacea* (Mello-Leitão, 1918) (type-species); *Gephyrellula lavidabonita* Galvis et al., 2024 and *Gephyrellula condeuba* sp. nov.

Distribution. *Gephyrellula* is a Neotropical genus, with records known from Colombia (Magdalena), all regions of Brazil, Argentina (Corrientes and Jujuy provinces) and Paraguay (Central, Paraguari e Itapúa) (Fig. 5).

Gephyrellula condeuba sp. nov.

https://zoobank.org/7A4F5CF3-B1D8-4B51-AB04-1E87F6CE0A90

Figs 1, 2A, 3, 4A

Type-material. ***Holotype*:** Brazil: • ♂; Bahia, Condeúba, Morro da Feirinha, 950 m altitude; 15°03'49"S, 42°09'23"W; 10–11.xi.2021; H. Schinelli, A. Prado, R. Baptista leg.; UFRJ 2418.

***Paratype*:** • ♀; Same data as holotype; UFRJ 2419.

Etymology. The specific name is a noun in apposition referring to the type-locality.

Diagnosis. The male of *G. condeuba* sp. nov. can be distinguished from those of *G. violacea* by the body covered by abundant dark grey spots and stripes, especially on legs and dorsum of abdomen (Fig. 1A), with carapace presenting black dots and stripes throughout, without white triangular mark (Fig. 1A) (vs. fewer dark spots throughout body and carapace with abundant black dots and stripes only on each side, with a wide median almost uniform light brown band and presence of a dirty white triangular marking on the posterior half of the cephalic area in *G. violacea*, see Santos and Rheims 2018, fig. 15); RTA wider and bifid, with sclerotized acute tips (Figs 1D, 2A) (vs. thin and with only one tip in G. violacea, Fig. 2B, also see Santos and Rheims 2018, figs 6, 7, 11, 12, 20, 21); VTA with a clearly convex ventral margin, presenting a basal flap (Figs 1D, 2A) (vs. VTA with straight ventral margin, Fig. 2B, also see Santos and Rheims 2018, figs 7, 12, 21); and PCA larger, distinctly hook-shaped (vs. PCA very small) (Fig. 1D–F, see Santos and Rheims 2018, figs 6, 8, 11, 12, 20, 21).

Females of *Gephyrellula condeuba* sp. nov. and *G. violacea* can be distinguished from *G. lavidabonita* (known only from the female holotype) by the MS wider than long (vs. longer than wide); pointed, elevated lobe of LP projecting over MS (vs. no lobe and MS covering posterior portion of LP);

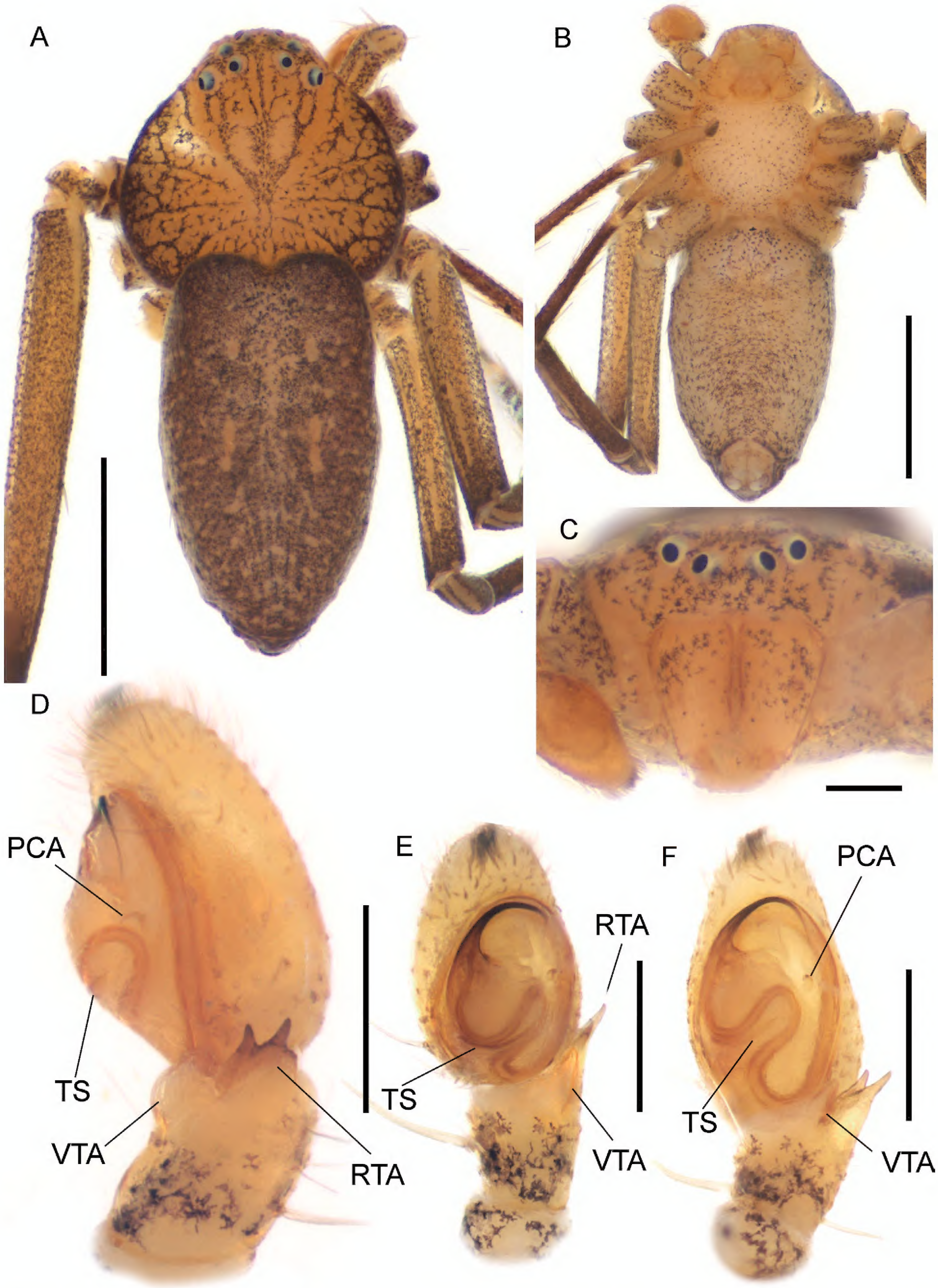

Figure 1. *Gephyrellula condeuba* sp. nov. holotype male. **A.** Habitus, dorsal view; **B.** Ventral view; **C.** Prosoma, frontal view; **D.** Palp, retrolateral view; **E.** Palp, ventral view centered on tibia; **F.** Palp, ventral view centered on tegulum. Abbreviations: PCA: Paraconductor apophysis; RTA: Retrolateral tibia apophysis; TS: Tegular suture; VTA: Ventral tibial apophysis. Scale bars: 1 mm (**A, B**); 0.2 mm (**C–F**).

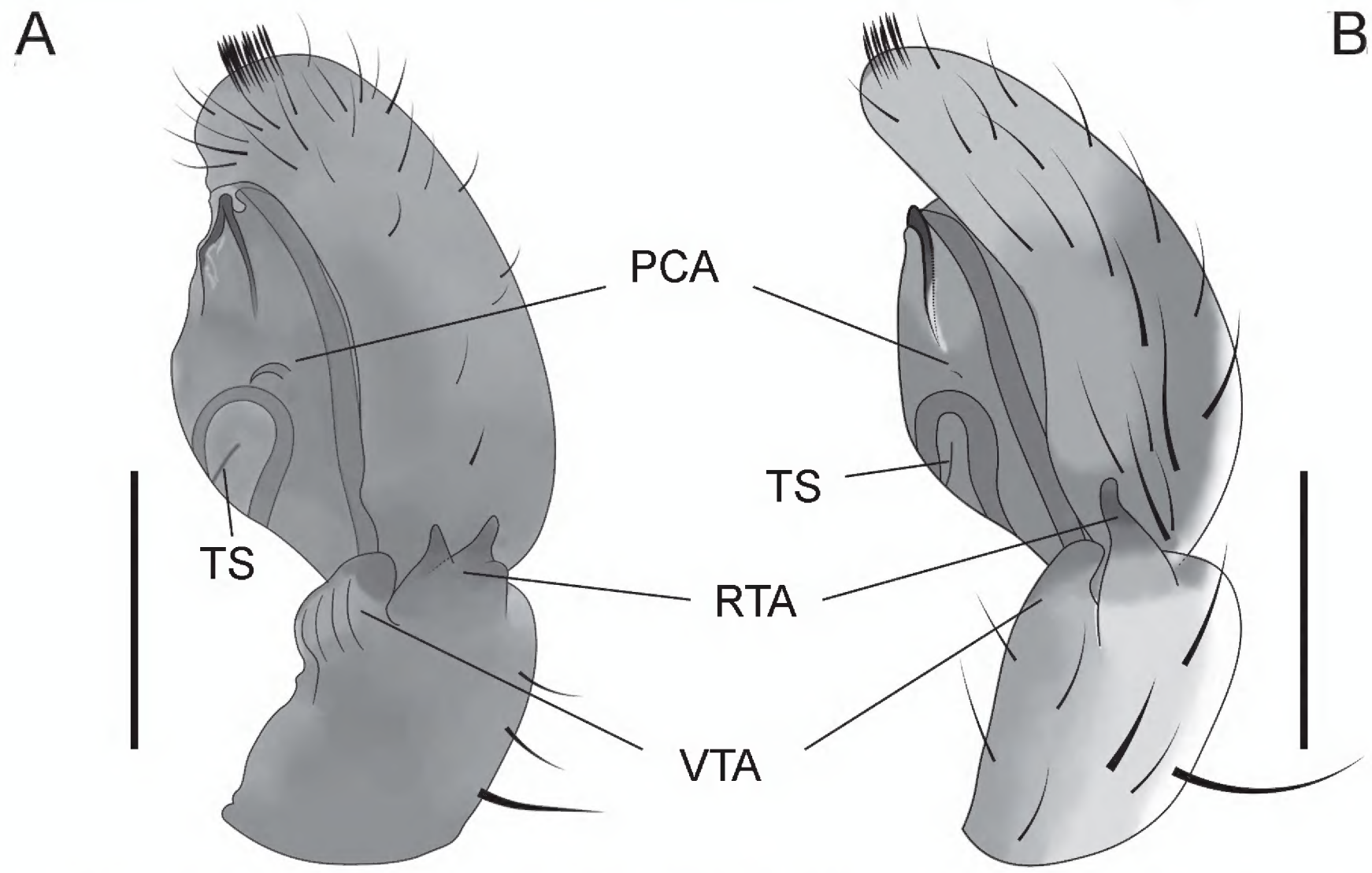

Figure 2. Male palp of *Gephyrellula* spp, retrolateral view. **A.** *Gephyrellula condeuba* sp. nov. holotype male (UFRJ 2418); **B.** *G. violacea* (UFRJ 2420/ENT6107).

and GP present (vs. absent). *Gephyrellula condeuba* sp. nov. females can be recognized from those of *G. violacea* by the absence of a distinct white triangular mark on the carapace (Fig. 3A) (vs. present in *G. violacea*, see Santos and Rheims 2018, fig. 17); median projection of LP very elevated from the plane of the epigyne as a clearly tridimensional fold, thinner and acute, not surpassing the margins of the MS (Figs 3D, 4A); GP longer, deeper and more conspicuous; and GH in a more horizontal position, clearly pointing to the ectal side and not surpassing the anterior margin of spermathecae (Figs 3D, 4A) (vs. median projection barely elevated from the plane of the epigyne, wide and rounded, clearly surpassing MS margins; GP shorter and shallow; and GH in a vertical position, pointing anteriorly and clearly surpassing the anterior margin of spermathecae, Fig. 4B, also see Santos and Rheims 2018, fig. 15, 23).

Description. Male (holotype UFRJ 2418). Total length: 3.04. Carapace 1.26 long, 1.37 wide; brownish yellow; suffused with black to dark gray irregular spots and radial bands extending from fovea to margins; with pair of non-pigmented areas over the cephalic sulcus; lateral margins almost uniformly black; with lateral row of bristles (most fallen, with only sockets left); flattened; wider than long (ca. 1.1×), wider at level of leg II, narrowed anteriorly, with maximum width ca. 3 times clypeus width; cephalic region also with black spots and bands, densely packed in eye area and forming a trident in its posterior half, slightly elevated and not distinctly separated by cephalic sulcus from the thoracic region. Clypeus low and vertical; shorter than MOQ; with sockets indicating presence of fallen macrosetae. Chelicerae with same color and pattern as carapace but fewer dark spots; with sparse setae (most lost in alcohol); fangs the same color as paturon; no visible teeth (but chelicerae were not dissected, making difficult the assessment of teeth presence). Labium and endites a little darker than sternum; labium wider than long with anterior margin rounded; endites longer than wide, oblong, angled inwards. Sternum pale yellow with dark grey irregular spots, fewer spots present in the anterior region behind the labium; anterior margin slightly concave; posterior margin round and convex, separating coxae IV by ca. 1.5 times their width. Eyes in two recurved rows; median quadrangle wider than long, wider posteriorly; median eyes of each row closer to lateral ones than to the other; white ocular veil present in all eyes. AME: 0.056, ALE: 0.051, PME: 0.048, PLE: 0.060. Interdistances: AME-AME: 0.14, AME-ALE: 0.45, ALE-PLE: 0.15, ALE-ALE: 0.29, PME-PME: 0.20, PME-PLE: 0.13, PLE-PLE: 0.52. MOQ width in anterior margin 0.22, posterior margin 0.29, length 0.24. Clypeus height: 0.118. Clypeus height index: 0.086.

Several legs missing in specimen, with only left leg II (but lacking tarsus and part of metatarsus) and right legs III and IV remaining. Leg II much longer than III and IV, which are almost of the same size. Trochantera, femora, and distal two-thirds of tarsi light brown; a little lighter ventrally, scattered with dark gray irregular spots. Patellae, tibiae, metatarsi, and basal third of tarsi mostly dark brown, with denser dark grey spots. Tarsus without visible spots at distal two-thirds; claw tufts present. Legs without scopula. Leg macrosetae pattern: Leg I without macrosetae. Femur II: d0-1-0, r0-1-1. Tibia II: v1-2-2, r0-0-1, p0-0-1. Femur III: d1-1-0. Tibia III: v0-2-0. Femur IV: d1-1-0. Tibia IV: v0-0-2. No spines on any patellae.

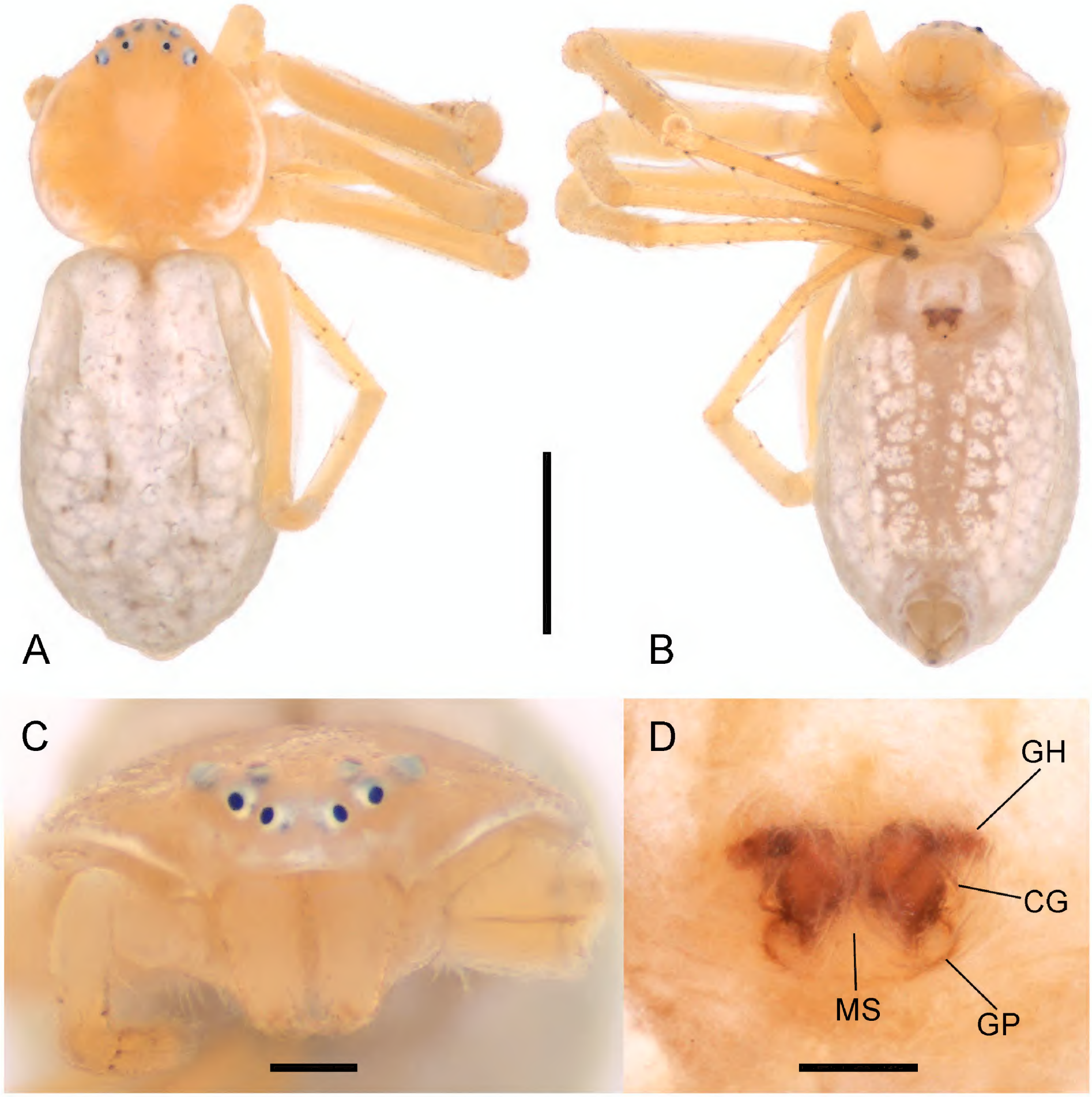

Figure 3. *Gephyrellula condeuba* sp. nov. paratype female. **A.** Habitus, dorsal view; **B.** Ventral view; **C.** Prosoma, frontal view; **D.** Epigyne, ventral view. Abbreviations: CG: Copulatory guides; GH: Glandular head; GP: Guide pockets; MS: Median septum. Scale bars: 1 mm (**A, B**); 0.2 mm (**C**); 0.1 mm (**D**).

Abdomen: dorsum with barely visible pale brown background, covered by densely packed black to dark grey spots and few subtle stripes. Cardiac area without spots delimiting its margins and with fewer spots. Small unpigmented patches spread over the dorsum, mostly at posterior third. Abdomen oval, longer than wide; with a deep notch in anterior margin. Two pairs of conspicuous dorsal sigillae, the second one elongated and subdivided, followed by two pairs of smaller depressions in the end of the median third. Venter pale yellow with abundant dark gray spots, not so dense as in dorsum. Spinnerets pale yellow, conical.

Palp: patella shorter than tibia, without apophysis. Tibia with 1 prolateral and 1 dorsal macrosetae, and 2 apophyses. VTA lamelliform, with middle and basal areas membranous and whitish yellow and lateral margins more sclerotized and darker; apical margins a little projected like a flap around a median concavity. VTA juxtaposed with RTA, with basal portion of its dorsal margin hidden by ventral crest of RTA. RTA bifid; sclerotized; with single broad base which narrows abruptly, originating two apical darker spiniform projections separated by a V-cleft, ventral one pointing straight up distally and with a thin curved crest connected to its basis, and dorsal one a little larger, slanted and pointing dorsally. Cymbium oblong, ca. 1.8 × longer than wide; with 1 prolateral macroseta and apical scopula of tenent setae. Tegulum elliptic, ca. 1.7 × higher than wide. Sperm duct clearly visible through tegument for most its extension;

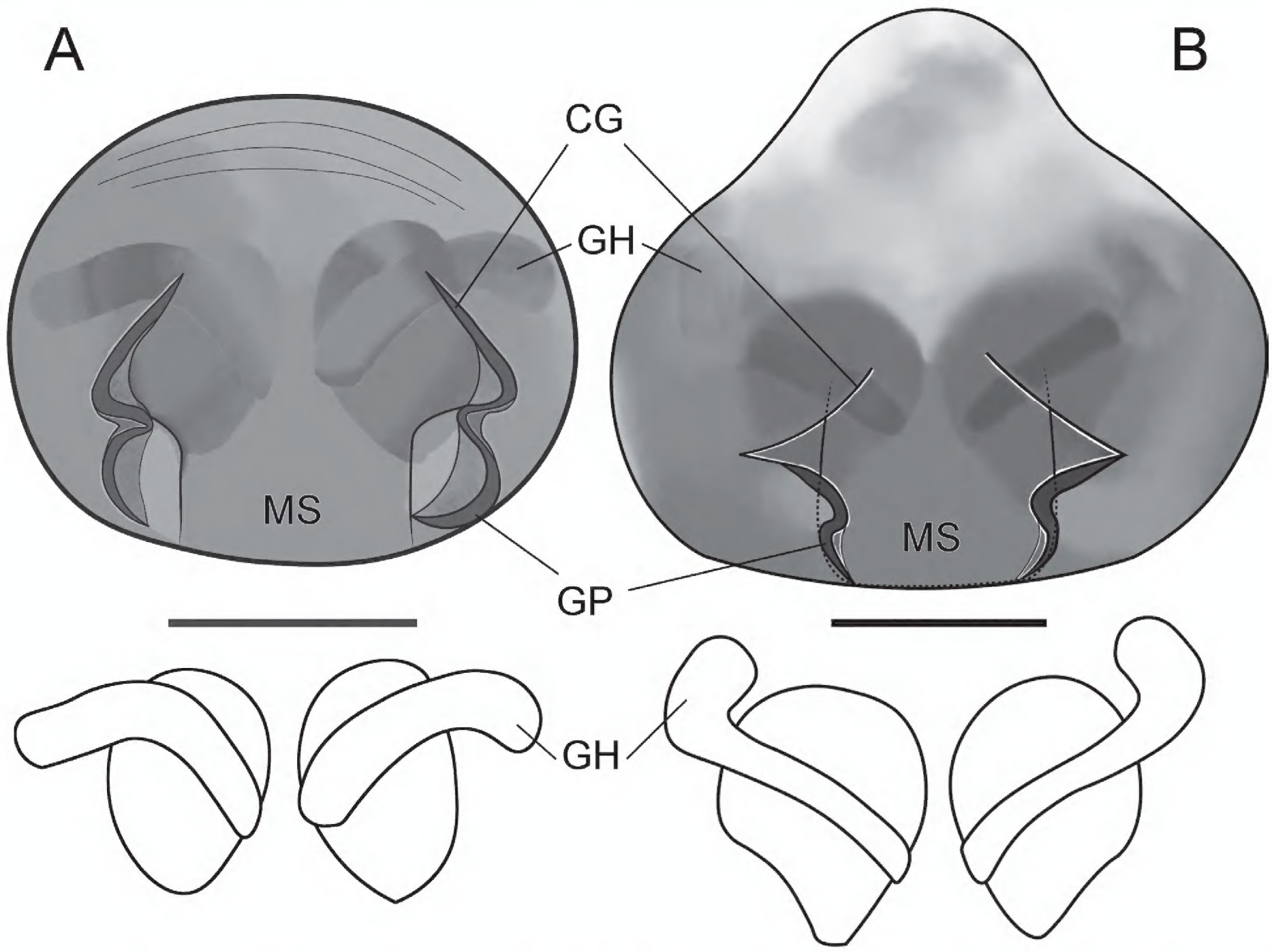

Figure 4. Female genitalia of *Gephyrellula* spp., top: ventral view of epigyne, bottom: outline of internal genitalia as seen through transparency of the epigyne in ventral view. **A.** *Gephyrellula condeuba* sp. nov. paratype female (UFRJ 2419); **B.** *G. violacea* (UFMG 619, specimen listed in the Material Examined by Santos and Rheims 2018).

extending along retrolateral margin of tegulum, rising from proximal margin forming large S-shaped tube with long tight median loop and much wider anterior one, with distal portion tapering and vanishing into embolus near prolateral margin. Tegular suture extending from outside apex of upper loop to inside the median loop. PCA small, but distinctly noticed and clearly hook-shaped, close to apex of median loop. Primary conductor absent. RMC not seen (but it may be small and translucent and visible only on Scanning Electron Microscopy as in *G. violacea*). Embolus filiform, describing a crooked curve, with strong reduction in diameter at its base and regularly tapering and getting paler towards its thin tip.

Female (paratype UFRJ 2419). Total length 3.52. General shape as in male, but with a much lighter coloration, lacking black or dark gray spots. Carapace 1.20 long, 1.30 wide; pale orange yellow with vaguely defined pale yellow triangular area at posterior half of the cephalic area; lateral margins with a white stripe, very thin anteriorly but increasing in size towards posterior margin, which lacks white pigment. Only sockets of lateral rows of bristles as in male. Chelicerae, labium, endites, and coxae with color similar to carapace. Sternum pale yellow, with thin dark contour through most of its extension. Eyes sizes: AME: 0.042, ALE: 0.040, PME: 0.038, PLE: 0.045. Interdistances: AME-AME: 0.14, AME-ALE: 0.04, ALE-PLE: 0.17, ALE-ALE: 0.29, PME-PME: 0.18, PME-PLE: 0.10, PLE-PLE: 0.50. MOQ width in anterior margin 0.20, posterior margin 0.25, length 0.21. Clypeus height: 0.114. Clypeus height index: 0.088.

Legs pale yellow, a little darker on inner side and at distal portion of metatarsi and whole tarsi; bearing small dark spots at macrosetae´s base. Legs without scopula. Leg macrosetae pattern: Tibia I: v1-2-2-1 (unaligned), r1-1-0. Metatarsus I: v2-2-2, r0-1-1. Leg II without spines. Tibia III: v0-2-2-0, r1-0-0 p1-0-0. Metatarsus III: v2-2-2, r1-1-0, p1-1-0. Tibia IV: v0-2-0. Metatarsus IV: v2-2-2, r1-0-0, p1-0-0. No spines on any patellae or femora. Leg measurements: Leg I: Total: 5.17 [Femur 1.55, Patella 0.63, Tibia 1.28, Metatarsus, 1.13 Tarsus: 0.58]. II: 5.05 [1.59, 0.59, 1.20, 1.01, 0.66]. III: 4.67 [1.50, 0.57, 1.13, 0.98, 0.49]. IV: 4.05 [1.39, 0.38, 0.96, 0.87, 0.45].

Abdomen 2.44 long, 1.46 wide. Dorsum covered by big white guanine spots, with slightly darker cardiac area, and scattered irregular gray and pale brown dots and streaks. Dorsal sigillae as in male. Venter with beige background covered by less dense guanine spots than dorsum, especially at anterior portion and median line. Spinnerets beige, conical.

Genitalia: Epigynal plate ca. 1.3 × wider than long; MS as wide as long, wider at anterior margin. CG long, transversely placed, beginning at the anterior area of

epigyne and just a bit posteriorly to anterior margin of main spermathecae and pointing ectally. GH in ectal position to spermatheca, not surpassing its anterior margin. Lateral plates projected as a thin, acutely pointed, elevated median lobe, separating the CG and the GP. GP longer than wide, regularly concave, with its anterior margin fused to the margin of the elevated lobe of the lateral plate; bearing a small concave excavation at its middle portion.

Note. Although males of *Gephyrellula* display usually more black pigment spread on the body than females, such as in *G. violacea* (see Santos and Rheims 2018, figs 1, 15–18), the amount of black pigment on the male holotype of *Gephyrellula condeuba* sp. nov. is unusually high (Fig. 1A–C). It is unclear whether the colour pattern of the holotype is a normal condition of the species or if it is a melanic specimen. Only additional specimens may answer that question.

Habitat. All specimens were collected by beating tree branches in a riparian forest around a small stream at Morro da Feirinha, around 950 m high. These riparian forests are small humid vegetation patches scattered in a large dry Cerrado region.

Distribution. Known only from the type locality in Condeúba, Bahia state, Brazil (Fig. 5).

Additional material examined. Brazil: **Bahia:** • 4juv.; Condeúba, Morro da Feirinha; 15°03"49'S, 42°09"23'W; 24.ii.2024; H. Schinelli leg.; UFRJ 2438.

Gephyrellula violacea (Mello-Leitão, 1918)

Gephyrella violacea Mello-Leitão, 1918: 122; Mello-Leitão 1929: 108 [♀].

Gephyrellula v.: Strand 1932: 137 (implicit combination through replacement name for genus).

Gephyrellula paulistana Soares, 1943: 10, figs 8, 9 [♂]. *Gephyrellula v.*: Santos and Rheims 2018: 382, figs 1–23 [♂♀, redescription, synonym with *G. paulistana*].

New records. Argentina: **Corrientes:** • 1♀; Ituzaingó, Islas Apipé Grande y Apipé Chico; 1945; W. Hanke leg.; MACN 1766 • 1♀ 2J; Esquina; 1999; L. A. Compagnucci leg; MACN 18574. **Jujuy:** • 1♀; Doctor Manuel Belgrano, Lagunas de Yala; 1949; N. Kormilev leg.; MACN 2751.

Brazil: **Rio de Janeiro:** • 1J; Rio de Janeiro, Cachoeiras de Macacu, Reserva Ecológica de Guapiaçu, Trilha São José; 12.vii.2018; G. Assunção leg.; UFRJ 2421. **Minas Gerais:** • 1♂ 1 J; Parque Nacional da Serra do Cipó, Trilha Mirante das Lagoas, Portaria Retiro; 03.xi.2021; A. W. do Prado, H. B. P. Schinelli, R. L. C. Baptista leg.; UFRJ 2420/ENT6107.

Paraguay: **Central:** • 1♀ 2J; Villeta; 30.viii.1984; J. A. Kochalka leg.; IBNP-Invert-JAK-CR 2574. **Itapúa:** • 1♀; Isla Yacyretá; 23.vi. 1994; J. A. Kochalka leg.; IBNP-Invert-JAK-CR 2576. **Paraguari:** • 1♀; Acahay; 21.iv.1984; J. A. Kochalka leg.; IBNP-Invert-JAK-CR 2575 • 1♀; Ybycuí National Park, Arroyo Corrientes; 4.ix.1984; J. A. Kochalka leg.; IBNP-Invert-JAK-CR 2577.

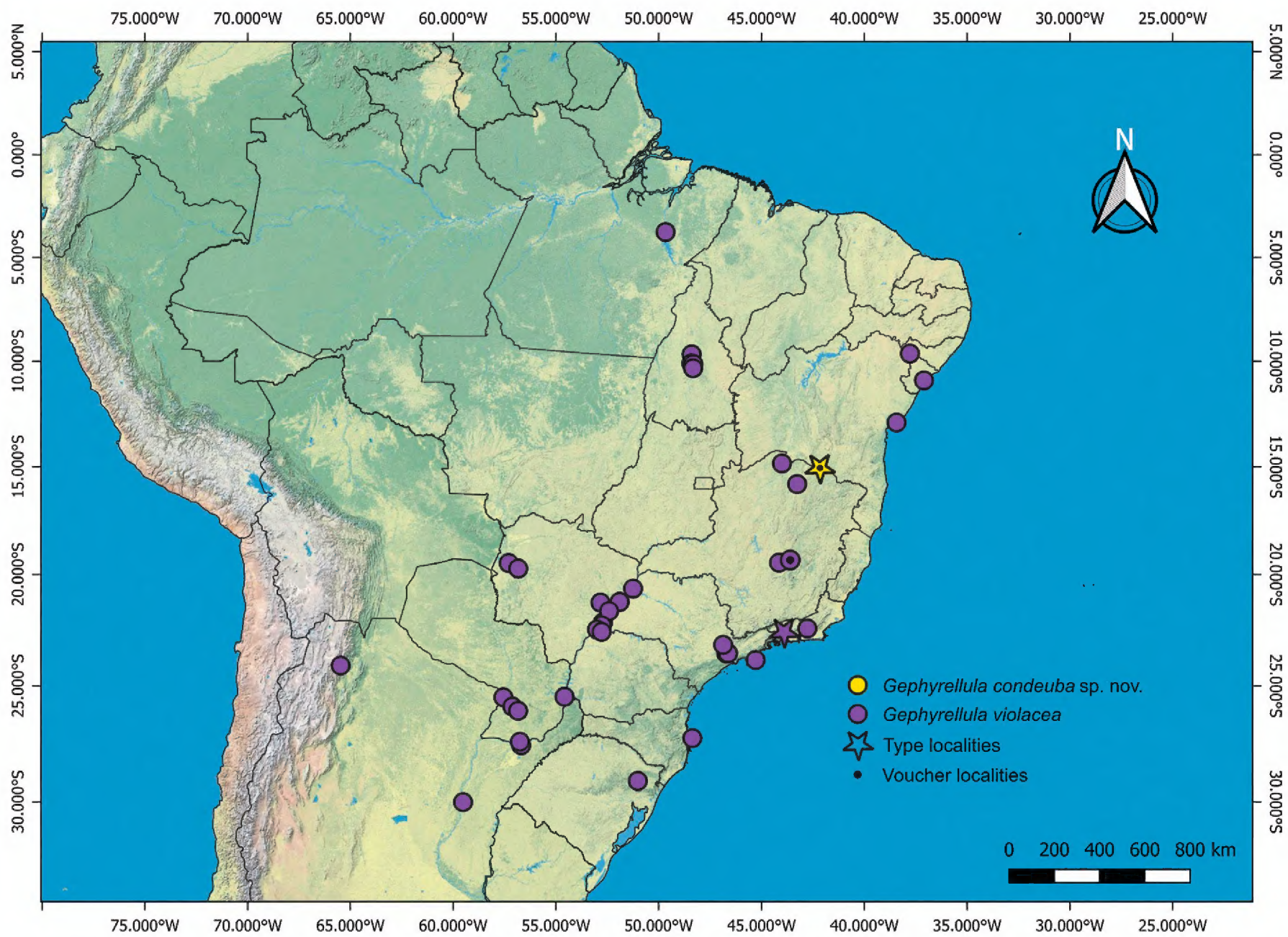

Figure 5. Distribution map of *Gephyrellula*, including records given by Santos and Rheims (2018) and new records. Type-localities are shown as stars, localities of voucher specimens of DNA sequences are shown with a dot in the middle. Records of *G. violacea* are in purple and *G. condeuba* sp. nov. in yellow.

Distribution. *G. violacea* is known from Argentina (Corrientes and Jujuy provinces), Paraguay (Central, Paraguari e Itapúa) and all regions of Brazil (Fig. 5).

Phylogeny

Results from ML and BI analyses were very similar (Fig. 6). Both analyses agree on the division of Philodromidae in two large groups, corresponding to the subfamilies Philodrominae (SH-aLRT/UFBoot=14.7/60 in ML; PP = 0.65 in BI) and Thanatinae (SH-aLRT/UFBoot=48/70 in ML; PP = 0.99 in BI).

In both analyses the two terminals of *Gephyrellula* were recovered together, with maximum support (PP = 1) in BI and near maximum (SH-aLRT/UFBoot=95.8/97) in ML. The position of *Gephyrellula* was also congruent, as member of a clade with other genera previously associated with the subfamily Philodrominae (*Petrichus*, *Philodromus*, *Pedinopistha*, and *Pagiopalus*) with moderate to high support (SH-aLRT/UFBoot=87.5/90 in ML; PP = 0.99 in BI).

Within this clade, both analyses recovered the grouping of the three species of *Philodromus* with high support (SH-aLRT/UFBoot=96.8/96 in ML; PP = 1 in BI), the two terminals of Hawaiian genera *Pedinopistha* and *Pagiopalus* with moderate to high support (SH-aLRT/UFBoot=86.2/84 in ML; PP = 0.91 in BI), and the two terminals of *Petrichus* with low to moderate support (SH-aLRT/UFBoot=78.9/57 in ML; PP = 0.68 in BI). This could possibly be partially explained by *Petrichus* sp. missing the COI marker while *P. marmoratus* is missing both 16S and H3. So, the two terminals only have the 28S marker in common for the analysis.

The relationships among the four abovementioned clades were not resolved in the BI analysis, which shows a polytomy with all four branches. In the ML analysis (Fig. 6), *Philodromus* was placed as the sister-group to the other three clades, and *Petrichus* appeared as sister to a clade formed by the Hawaian genera + *Gephyrellula*.

Discussion

Comparative diagnosis and phylogenetic placement

Santos and Rheims (2018) pointed similarities between *Gephyrellula* and the *Ebo*-like philodromids *sensu* Muster (2009), namely AME larger than all other eyes, median eyes of each row closer to lateral ones than to the other, and elongated leg II. However, we cannot rely on those characters alone to place *Gephyrellula* close to *Ebo* and related genera, since there is a lot of variation in eye placement in Philodromidae, and a longer leg II is found in most genera. *Gephyrellula condeuba* sp. nov. does not have AME larger than all other eyes, but instead the PLE is larger in both sexes (PLE > AME > ALE > PME), and only the male has a longer leg II, while leg I is the longest in the female. Even in *G. violacea*, the measurements given by Santos and Rheims (2018) show that only females have AME larger than the PLE (AME > PLE > ALE = PME), while males have both eyes of similar size and larger than others (PLE = AME>ALE > PME), which is arguably the same case found in *G. condeuba* sp. nov., whose PLE are larger than AME only by a negligible amount. Despite those deviations of the characters given by Santos and Rheims (2018), the diagnostic features from each genus remain useful: *Gephyrellula* is separated from *Halodromus* and *Rhysodromus* by the leg scopula absent and the clypeus index (clypeus height/carapace width, which is 0.09 in *G. condeuba* sp. nov.); from *Ebo* by the presence of lateral spines on tibiae and metatarsi I and II and the well-developed VTA and RTA in male palp; and from *Titanebo* by the presence of a small hook-shaped PCA in male palp.

As discussed by Santos and Rheims (2018), the original description of *Gephyrellula* states that it is similar to *Gephyra* (L. Koch, 1875) [currently *Gephyrota* Strand, 1932] and *Gephyrina* Simon, 1895 due to their flat body. Both *Gephyrina* and *Gephyrota* are poorly delimited genera, so no taxonomic decisions regarding them can be made at the moment.

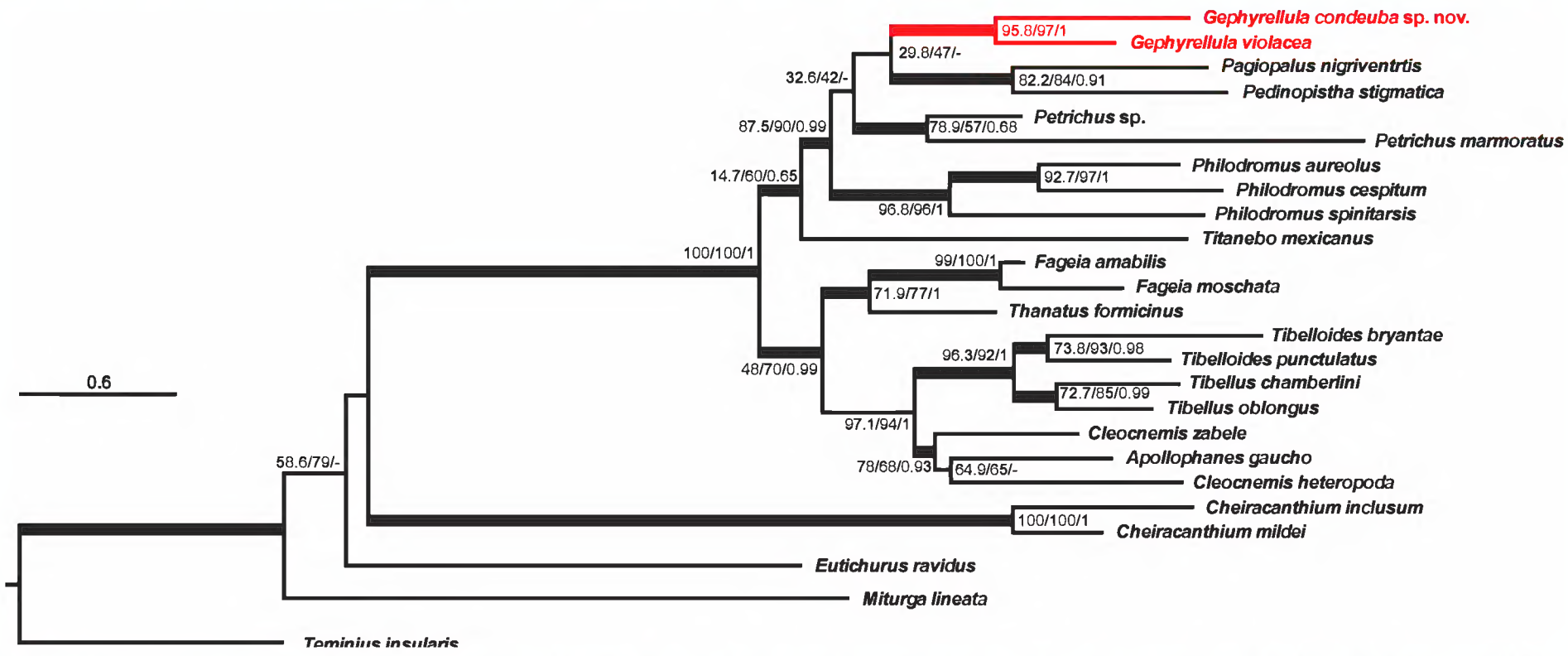

Figure 6. Maximum likelihood tree of Philodromidae and outgroups based on four molecular markers (COI, H3, 16S, and 28S). Internal branches recovered also in Bayesian inference analyses are thickened. The clade including both terminals of *Gephyrellula* is shown in red. Clade support associated to each node are SH-aLRT/UFBoot/Bayesian posterior probabilities.

However, photos of *Gephyrota glauca* (Jézéquel, 1966) in Dippenaar-Schoeman et al. (2022) show that it is indeed very similar to *Gephyrellula* in general morphology, although the epygine is clearly different. The only other species among this group with available information is *Gephyrina imbecilla* Mello-Leitão, 1917, which was synonymized with "*Cleocnemis*" *mutilata* (Mello-Leitão, 1917) by Prado et al. (2022). The illustration of the holotype in the redescription of *Gephyrina imbecilla* (Mello-Leitão 1929, fig. 32) shows a color pattern very different from those found in *Gephyrellula*; and the palp morphology described by Prado et al. (2022), with a Ventral Bulbar Apophysis (VBA) forming prominent tegular scutum and a very large sinuous PCA, is also very different from *Gephyrellula* palps, which have no VBA and bear a small hook-shaped PCA.

Previously, the only phylogeny including any terminal of *Gephyrellula* was the molecular phylogeny of Prado et al. (2022), which placed *Gephyrellula* in two different positions according to the particular analysis made. In the maximum likelyhood (ML) tree, *Gephyrellula* was recovered together with the Hawaiian species *Pedinopistha stigmatica* (Simon, 1900), while *Pagiopalus nigriventris* Simon, 1900 was the sister-group of both. *Gephyrellula* species share with *Pedinopistha* male palps with a small PCA (Suman 1971, figs 123, 128, 133, 138), with *G. condeuba* sp. nov. also sharing the RTA bidentate. However, *Pedinopistha* has a MOQ much wider than long and a very wide clypeus, with the anterior margin over half the width of the widest portion of the carapace (Suman 1971: 852), while species of *Gephyrellula* have clypeus around a third of the width of the carapace and the MOQ only slightly wider than long. The other Hawaiian genus, *Pagiopalus*, has the clypeus width and MOQ proportions more similar to those of *Gephyrellula* (Suman 1971: 842), but the two can be distinguished by characteristics of the male palp, as the tegular suture (small vs. long), median loop of the reservoir (small vs. long), and PCA (usually absent vs. present); and female epigyne, as projected lobes of LP (absent vs. usually present) (see Suman 1971, figs 102–121). In the Bayesian inference (BI) tree, *Gephyrellula* was recovered as sister to a clade composed by "*Cleocnemis*" *mutilata*, *Philodromus cespitum* (Walckenaer, 1802) and *Philodromus aureolus* (Clerck, 1757), with *Philodromus spinitarsis* Simon, 1895 as sister to all of these (Prado et al. 2022). The proximity to "*Cleocnemis*" *mutilata* (synonym of *Gephyirina imbecilla*) in this phylogeny agrees with the idea of Mello-Leitão (1918) that *Gephyrellula* is close to *Gephyrina*, though they can be easily distinguished by the characters mentioned above. Besides the flat body and longer leg II, they share the presence of white veils around their eyes, which is also present in *P. aureolus* (Zhang et al. 2022, fig. 193A, B) and *P. cespitum* (Zhanget al. 2022, fig. 194A, B), but not in *P. spinitarsis* (Zhanget al. 2022, fig. 197A, B).

As expected from the very similar datasets, our phylogeny agrees with most of the main results of Prado et al. (2022). In both studies, Philodromidae is divided into two subfamilies, Thanatinae and Philodrominae, but while the genus *Titanebo* was recovered as sister group to the two subfamilies in Prado et al. (2022), in our analysis it was recovered closer to Philodrominae, albeit with low support. This positioning agrees with Wheeler et al. (2017), Griotti et al. (2022), and the original definition of the group proposed by Schick (1965).

Conclusion

With the new terminal and markers added for *Gephyrellula*, some uncertainties are resolved while others remain. In both studies the genus was placed within the Philodrominae, among the genera *Petrichus*, *Philodromus*, *Pedinopistha*, and *Pagiopalus*, but relationships among these genera remain uncertain. In our analyses, the position of *Gephyrellula* differs from both the ML and BI analyses of Prado et al. (2022). It is not placed inside the Hawaiian clade containing *Pagiopalus* and *Pedinopistha*, as opposed to the previous ML phylogeny; and it is not placed among the three *Philodromus* species (which are grouped here as a clade in both analyses with high support), as opposed to the previous BI phylogeny. So while the two analyses of Prado et al. (2022) suggested that *Gephyrellula* was part of either the Hawaiian clade or the *Philodromus* genus, our main phylogenetic result is its placement as a lineage separated from the others in the subfamily Philodrominae. However, further studies with additional molecular data from terminals of *Ebo*, *Titanebo* and other Neotropical philodromids with little information available, are still needed to define which group is its closest relative, as well as to further decipher the relationships among this subfamily.

Funding

HBPS is supported by a doctoral fellowship from Coordenação de Aperfeiçoamento de Pessoal de Nível Superior. DMT is a research productivity fellow from Conselho Nacional de Desenvolvimento Científico e Tecnológico (CNPq Proc. 314557/2021-0) and a Cientista do Nosso Estado fellow from Fundação Carlos Chagas Filho de Amparo à Pesquisa do Estado do Rio de Janeiro (FAPERJ Proc. E-26/202.672/2019).

Acknowledgments

Authors would like to thank Gabriel Assunção Oliveira, who participated in the second field trip to the type locality Condeúba, Bahia, Brazil; Clara Guimarães for making the distribuition map; and curators Martín Ramírez, for receiving author AWP in a visit to the MACN collection, and John Kochalka, for loaning specimens.

References

Anisimova M, Gil M, Dufayard JF, Dessimoz C, Gascuel O (2011) Survey of branch support methods demonstrates accuracy, power, and robustness of fast likelihood-based approximation schemes. Systematic Biology 60(5): 685–699. https://doi.org/10.1093/sysbio/syr041

Dippenaar-Schoeman AS, Haddad CR, Foord SH, Lotz LN (2022) The Philodromidae of South Africa. Version 2. South African National Survey of Arachnida Photo Identification Guide, Irene, 53 pp.

Dondale CD, Redner JH (1978) The insects and arachnids of Canada, Part 5. The crab spiders of Canada and Alaska, Araneae: Philodromidae and Thomisidae. Research Branch Agriculture Canada Publication 1663: 1–255. https://wsc.nmbe.ch/reference/5001

Dupérré N (2023) Araneae (spiders) of South America: a synopsis of current knowledge. New Zealand Journal of Zoology 50(1): 3–117. https://doi.org/10.1080/03014223.2021.2022722

Galvis W, Casas CM, Villareal E, Sherwood D (2024) Running crab spiders (Araneae: Philodromidae) from Colombia: new species and records. Arachnology 19(8): 1127–1138. https://doi.org/10.13156/arac.2024.19.8.1127

Griotti M, Grismado CJ, Roig-Juñent S, Ramírez MJ (2022) Taxonomy and phylogenetic analysis of the South American genus *Petrichus* Simon (Araneae: Philodromidae) provide new insights into the running crab spiders' phylogeny. Invertebrate Systematics 36(4): 306–353. http://dx.doi.org/10.1071/IS21068

Hoang DT, Chernomor O, von Haeseler A, Minh BQ, Vinh LS (2018) UFBoot2: Improving the ultrafast bootstrap approximation. Molecular Biology and Evolution 35: 518–522. https://doi.org/10.1093/molbev/msx281

Homann H (1975) Die stellung der thomisidae und der philodromidae im system der araneae (Chelicerata, Arachnida). Zeitschrift für Morphologie der Tiere 80(3): 181–202. https://doi.org/10.1007/BF00285652

Kalyaanamoorthy S, Minh BQ, Wong TKF, von Haeseler A, Jermiin LS (2017) ModelFinder: fast model selection for accurate phylogenetic estimates. Nature Methods 14(6): 587–589. https://doi.org/10.1038/nmeth.4285

Mello-Leitão CF de (1918) Un genero novo de Thomisidas da sub-familia Philodrominae. Revista da Sociedade Brasileira de Sciencias 2: 121–123. https://wsc.nmbe.ch/reference/1749

Mello-Leitão CF (1929) Aphantochilidas e Thomisidas do Brasil. Arquivos do Museu Nacional do Rio de Janeiro 31: 9–359. https://wsc.nmbe.ch/reference/2022

Muster C (2009) The Ebo-like running crab spiders in the Old World (Araneae, Philodromidae). ZooKeys 16: 47–73. https://doi.org/10.3897/zookeys.16.230

Nguyen LT, Schmidt HA, von Haeseler A, Minh BQ (2015) IQ-TREE: A fast and effective stochastic algorithm for estimating maximum likelihood phylogenies. Molecular Biology and Evolution 32: 268–274. https://doi.org/10.1093/molbev/msu300

Pantoja P, Drago-Bisneto M, Saturnino R (2020) Updates on Berlandiella (Araneae: Philodromidae): a new species, description of the male of *B. querencia* and new diagnosis for the genus. Zoologia 37: 1–13. https://doi.org/10.3897/zoologia.37.e37384

Prado AW, Baptista RLC, Schinelli HBP, Takiya DM (2022) Solving a running crab spider puzzle: delimiting Cleocnemis Simon, 1886 with implications on the phylogeny and terminology of genital structures of Philodromidae. BMC Zoology 7(51): 1–35. https://doi.org/10.1186/s40850-022-00136-7

Ramírez MJ (2014) The morphology and phylogeny of dionychan spiders (Araneae: Araneomorphae). Bulletin of the American Museum of Natural History 390: 1–374. https://doi.org/10.1206/821.1

Ronquist F, Teslenko M, Van Der Mark P, Ayres DL, Darling A, Höhna S, Larget B, Liu L, Suchard MA, Huelsenbeck JP (2012) MrBayes 3.2: Efficient Bayesian Phylogenetic Inference and Model Choice Across a Large Model Space. Systematic Biology 61(3): 539–542. https://doi.org/10.1093/sysbio/sys029

Santos FH, Rheims CA (2018) Taxonomic revision of the genus *Gephyrellula* Strand, 1932 (Arachnida, Araneae, Philodromidae). Zootaxa 4527(3): 381–391. https://doi.org/10.11646/zootaxa.4527.3.7

Schick, RX (1965) The crab spiders of California (Araneae, Thomisidae). Bulletin of the American Museum of Natural History 129(1): 1–180. https://wsc.nmbe.ch/reference/3754

Schinelli HBP, Massim J, Prado AW, Teixeira RA, Baptista RLC (2024) Taxonomic revision of the elusive Neotropical running crab spider genus *Fageia* Mello-Leitão, 1929 (Araneae, Philodromidae). Zoological Research: Diversity and Conservation 1(3): 204–225. https://dx.doi.org/10.24272/j.issn.2097-3772.2024.004

Schwarz G (1978) Estimating the dimension of a model. The Annals of Statistics 6: 461–464. https://doi.org/10.1214/aos/1176344136

Soares BM (1943) Novos thomisidas brasilieros. Papéis Avulsos de Zoologia, Sao Paolo 3: 1–18. https://wsc.nmbe.ch/reference/2715

Strand E (1932) Miscellanea nomenclatorica zoologica et palaeontologica, III, IV. Folia Zoologica et Hydrobiologica, Rigā 4: 133–147, 193–196. https://wsc.nmbe.ch/reference/2139

Suman TW (1971) Spiders of the family Thomisidae in Hawaii. Pacific Insects 12: 773–864. https://wsc.nmbe.ch/reference/4174

Wheeler WC, Coddington JA, Crowley LM, Dimitrov D, Goloboff PA, Griswold CE, Hormiga G, Prendini L, Ramírez MJ, Sierwald P, Almeida-Silva L, Alvarez-Padilla F, Arnedo MA, Silva LRB, Benjamin SP, Bond JE, Grismado CJ, Hasan E, Hedin M, Izquierdo MA, Labarque FM, Ledford J, Lopardo L, Maddison WP, Miller JA, Piacentini LN, Platnick NI, Polotow D, Silva-Dávila D, Scharff N, Szűts T, Ubick D, Vink CJ, Wood HM, Zhang J (2017) The spider tree of life: phylogeny of Araneae based on target-gene analyses from an extensive taxon sampling. Cladistics 33(6): 574–616. https://doi.org/10.1111/cla.12182

World Spider Catalog (2025) World spider catalog, version 26.0. Natural History Museum Bern. https://wsc.nmbe.ch/

Zhang F, Peng JY, Zhang BS (2022) Spiders of Mt. Xiaowutai. Science Press, Beijing, 387 pp. https://wsc.nmbe.ch/reference/16848

Supplementary material 1

Sequences newly generated for this study

Authors: Hector Baruch Pereira Schinelli, André Wanderley do Prado, Renner Luiz Cerqueira Baptista, Daniela Maeda Takiya

Data type: docx

Explanation note: Specimen voucher codes, collecting locality (country and state), and GenBank accession codes for each of the markers used are given.

Copyright notice: This dataset is made available under the Open Database License (http://opendatacommons.org/licenses/odbl/1.0). The Open Database License (ODbL) is a license agreement intended to allow users to freely share, modify, and use this Dataset while maintaining this same freedom for others, provided that the original source and author(s) are credited.

Link: https://doi.org/10.3897/evolsyst.9.143758.suppl1